A Compact Coaxial Waveguide Combiner Design For Broadband Power Amplifiers

Pengcheng Jia, Robert A. York

E.C.E. Dept., University of California, Santa Barbara, CA 93106, USA

***Abstract* — We report an enhanced broadband passive combiner structure using a dense slot-line antenna array in an oversized coaxial waveguide. A significant reduction in size has been achieved while maintaining a 6-18GHz bandwidth and capacity for 32 MMIC amplifiers. A broadband slotline to microstrip line transition is developed and monolithically integrated with the slot-line antennas, to eliminate a troublesome bond-wire transition in earlier design and provide better compatibility with commercial MMICs. The Spectral Domain Method (SDM) is applied to compute the field in the structure, and small reflection theory is extended to synthesize the waveguide taper and optimized slotline taper array.**

I. INTRODUCTION

Waveguide-based spatial power combiners using finline arrays are good candidates for high power broadband combining [1-2]. In this approach, the combiner is implemented in a "tray" architecture, which permits the use of broadband antennas and improved functionality through circuit integration along the direction of propagation. Each tray consists of a number of tapered slotline or finline transitions, which coupled energy to and from a waveguide aperture to a set of MMIC amplifiers.

A rectangular waveguide power combiner has achieved 120-Watt output power over X-Band [1]. However, the bandwidth of rectangular waveguide combiners is limited by the cutoff frequency of the waveguide. To fully exploit the inherently wide bandwidth of a slotline antenna array, a coaxial waveguide combiner is developed. In this case the slotline array is loaded radially inside the opening of an oversized coaxial waveguide. Preliminary results demonstrated over 12 GHz bandwidth in a prototype passive structure [3]; this was subsequently integrated with 32 broadband traveling-wave amplifier MMICs [4], demonstrating high combining efficiency of >75%.

As shown in Fig. 1, the center section of the coaxial waveguide combiner is enlarged to accommodate the slotline array and MMICs. Coaxial waveguide tapers are applied at both ends of the center section, providing transition from the enlarged center section to standard N connectors. Our previous design was undesirably large in both the diameter of the center section and the length of waveguide taper. A new compact system, which provides the same performance as the larger one, was developed and reported here.

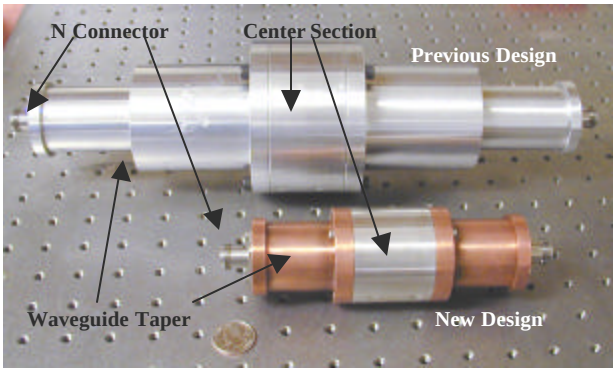

Fig. 1. Comparison between previous design and the new compact design.

For low power demonstrations, the MMICs were die-attached directly to the AlN substrate supporting the slot-line antennas. But the MMICs must be attached to the metal carrier for better thermal management in high power modules, as in [1]. A slotline to microstrip line transition is therefore necessary for connection between slotline antenna and the commercial MMICs. In [1-2], a separate microstrip line was bonded to the end of slotline with hybrid wire bonding. The wire bonding adds parasitic inductance to the transition, and increase the difficulty in fabricating the system. A monolithic broadband transition is developed in this paper to eliminate the parasitic effect. The new transition can retain the same bandwidth. Furthermore, it can be easily extended to higher frequencies.

II. COAXIAL WAVEGUIDE DESIGN

The primary goal of the work is to re-engineer the combiner to minimize the physical size, while maintaining a large amplifier capacity, wide bandwidth (6-18GHz is the goal), and good thermal capacity. We succeed in reducing the diameter of the center section from 4 inch

0-7803-6540-2/01/$10.00 (C) 2001 IEEE

to 2.2 inch, and the length of each waveguide taper from 6.2 inch to 2.2 inch.

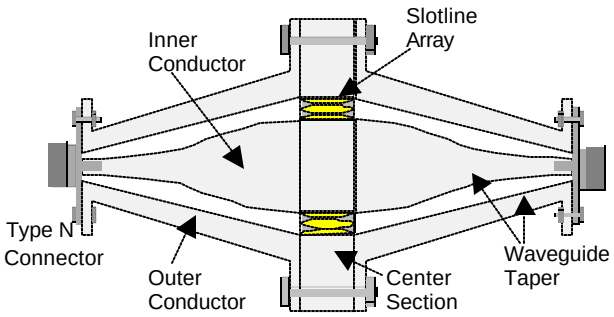

Fig. 2. Cross section of loaded coaxial waveguide combiner.

When slotlines are loaded in the waveguide, as shown in Fig. 2, the input impedance of each slotline is the number of channels times the waveguide impedance. Lower waveguide impedance leads to smaller waveguide aperture, which is helpful in suppressing higher modes, and also can keep the slotline taper shorter, which means lower conductive loss. Thus the impedance of the center section was chosen to be 30 Ohm, with outer and inner diameter of the coaxial waveguide opening to be 1.6 and 0.96 inch.

The reflection from the N-connector to flared waveguide line is minimized by the optimized coaxial waveguide transition. The gradual waveguide taper is synthesized from small reflection theory of TEM lines [5], and has an input reflection coefficient

$$\Gamma_{in}(f) = \frac{1}{2}\int_0^{q_t} e^{-jq}\,\frac{d}{dq}\ln\left(\frac{Z(q)}{Z_0}\right)dq\,. \qquad (1)$$

where b is the propagation constant, $q = 2b\,dz$ is the round-trip phase delay to a point z along the taper, L is the taper length, and $q_t = 2bL$. In order to maintain an input reflection coefficient $\Gamma < \Gamma_m$ over the desired bandwidth, it has been shown in [5,6] that $Z(q)$ must take the form

$$\ln\frac{Z(q)}{Z_0} = \frac{1}{2}\ln\frac{Z_L}{Z_0} + \Gamma_m A^2 F\left(\frac{2q}{2q_t} - 1, A\right). \qquad (2)$$

The simulation and measurement results of the unloaded compact coaxial waveguide are shown in Fig. 3. There is no solder or epoxy used in assembling the system. The center conductor of the combiner is designed to mate directly to the center conductor of a type-N connector for easy assembly, but this also introduced additional loss and reflection. And 2 N-to-SMA connectors are used for measurement, which is not considered in simulation. The loss and reflection of the N-to-SMA connector is also shown in Fig. 3. It contributes to the discrepancy between simulation and measurement.

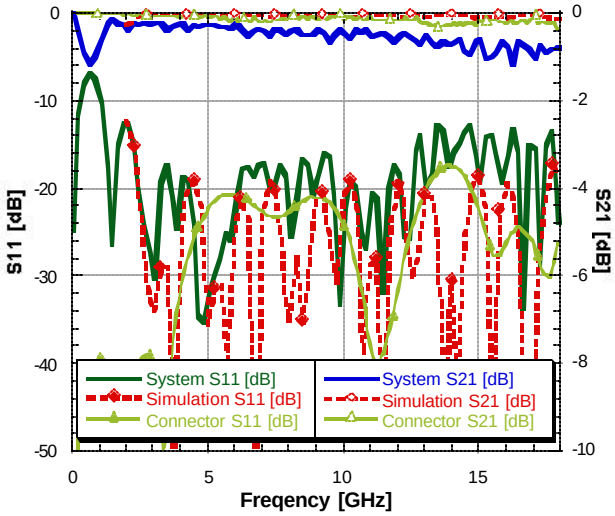

Fig. 3. S parameter of unloaded coaxial waveguide.

III. Synthesis of Waveguide Slotline Array

16 slotline circuit cards will be radially loaded inside the center waveguide opening. The symmetry and the thinness of circuit substrate allow us to focus analytical attention on a 1/16th units cell. The 1/16th cell is further approximated by a parallel-plate waveguide [3]. The Spectral Domain Method is applied to compute the field. Then the propagation constant and impedance are calculated by an iteration process. Again the small reflection theory is used to optimize the slotline taper, with b as a function of the slotline gap and frequency. The detailed modeling work is elaborated in [4]. The layout of the slotline taper is shown in Fig. 4.

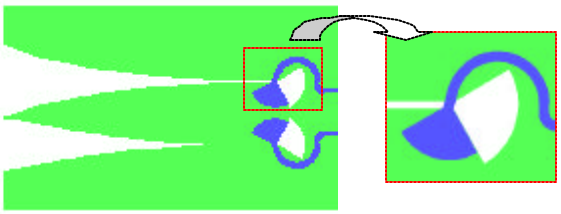

Fig. 4. Layout of the slotline taper and the slotline to microstrip line transition.

Each circuit tray carries 2 slotline tapers. To improve the linearity of the combiner, power should be distributed evenly to each taper. But the field inside the waveguide is not radially uniform. So each of the 2 slotline tapers on each tray is designed with a different slot opening to equalize the power. When we put the slotline tray inside the waveguide, they will have the same outer radius to inner radius ratio.

IV. SLOTLINE TO MICROSTRIP LINE TRANSITION

In the previous design, a separate microstrip transition was adopted to provide connection from the end of slotline to MMICs. The microstrip line and slotline were not in the same plane, bonding wire was needed for interconnection. It is hard to keep the wire very short in fabrication. To avoid parasitic inductance, a monolithic slotline to microstrip transition is employed in the new design [7].

As shown in Fig. 5, the slotline is processed on the back of the AlN substrate, with a 90-degree slotline short stub at the end. A 90-degree microstrip open stub is aligned to the slotline stub on the top of the substrate. The center of the 2 stubs are on the same line perpendicular to the surface, and their edges are parallel to each other. When put onto a metal carrier, the slotline become the ground of microstrip line, which is also the ground of MMICs. Due to the space limitation inside the compact structure, the stubs have to be bended 15-degree inwards, and the microstrip line detours around the slotline stub in a small loop.

The transition in Fig. 4 is modeled in Fig. 5.

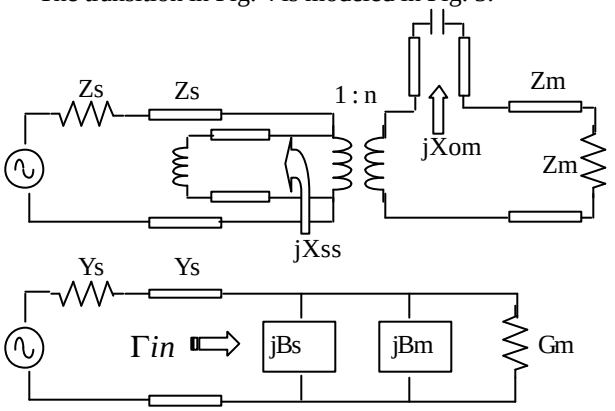

Fig. 5. Circuit model of slotline to microstrip line transition.

The short slotline stub and open microstrip stub can be treated as a series of straight sections of various widths that are cascaded together [8]. To improve the accuracy of structure enclosed in waveguide, we use 3D simulator Agilent HFSS to compute the reactance of the slotline stub jXss and microstrip stub jXom. Then we apply the values into the circuit model and optimize other parameters in the transition. In the circuit model, Zm and Zs is the characteristic impedance of microstrip line and slotline, n is the transformer ratio,

$$n = -\frac{1}{Vo}\int_{-\frac{b}{2}}^{\frac{b}{2}} Ey(h)dy,$$

$$Ey(h) = -\frac{Vo}{b}\left(\cos\frac{2pu}{lo}h - \cot q_o \sin\frac{2pu}{lo}h\right),$$

$$Gm = \frac{n^2 Zm}{Zm^2 + Xom^2}, \qquad Ys = \frac{1}{Zs}, \tag{3}$$

$$Bm = -\frac{n^2 Xom}{Zm^2 + Xom^2}, \qquad Bs = -\frac{1}{Xss}.$$

Vo is the voltage across the slot and *Ey(h)* is the electric field of the slotline on the other surface of the substrate. The details of the calculation of n are in [9]. The reflection coefficient can be expressed as:

$$\Gamma in = \frac{Ys - Gm - j(Bs + Bm)}{Ys + Gm + j(Bs + Bm)}. \tag{4}$$

Our goal is to achieve bandwidth from 6 to 18GHz. Simulation shows that the lower band is more sensitive to the parameters. So we choose 10GHz as the center frequency, then optimize the transition at this frequency to satisfy *Ys=Gm*, and *Bs=-Bm*.

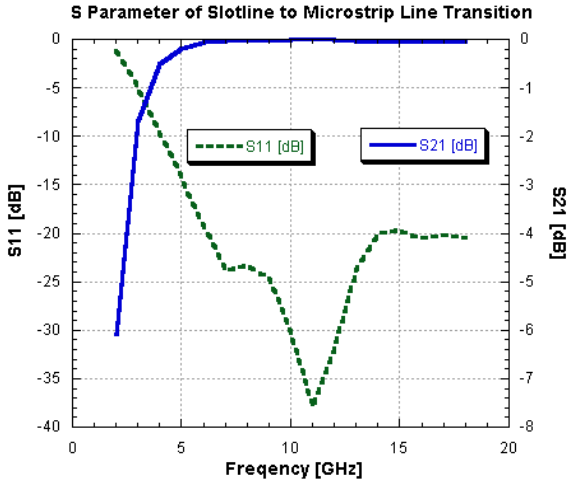

Fig. 6. S parameters of slotline to microstrip line transition from Agilent HFSS simulation.

The microstrip line is fixed to be 50 Ohm, corresponding to 278 um strip width on a 254 um thick AlN substrate. The characteristic impedance of the slotline times n^2 should be close to 50 Ohm. We choose the width of the slotline to be 40 um to match Ys with Gm. Due to the limitation of the space inside the waveguide structure, the radius of the slotline stub is selected to be 2000 um. To realize Bs=-Bm and minimize the reflection coefficient, the microstrip open stub should have a radius of 1500 um. Further optimization with Agilent HFSS shows that microstrip stub with 1600 um radius have a wider bandwidth. Simulation result, which is shown in Fig. 6, indicates that the slotline to microstrip transition can achieve a bandwidth of 12 GHz, from 6 to 18 GHz. If scaled down properly, the transition can also work at higher bands. The parasitic effect is much smaller than the bonding wire connection used in earlier work.

V. Compact Passive Structure of Coaxial Waveguide Combiner

Fig. 7 shows the open view of the combiner loaded with 16 circuit cards for loss measurement that is shown in the lower left corner. Each circuit card has 2 transitions placed back to back. Slots are machined along the walls of the center flared coaxial waveguide, and circuit cards are slid into it. The performance of the overall system, which includes waveguide tapers, a divider and a combiner, is shown in Fig. 8 6-18 GHz bandwidth can be observed from both the simulation and the measurement. The discrepancy most comes from the connectors, which introduce more than 1 dB loss at the higher band. The loss can be reduced by improved connections.

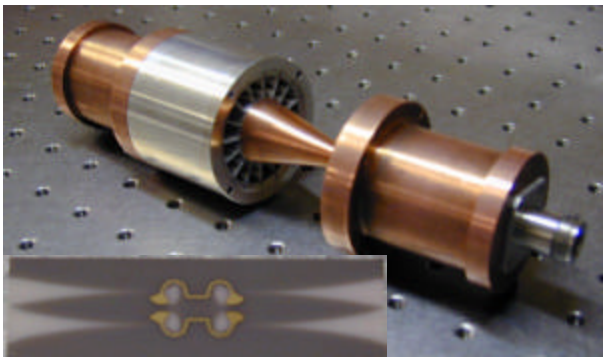

Fig. 7. Open view of the passive coaxial waveguide combiner.

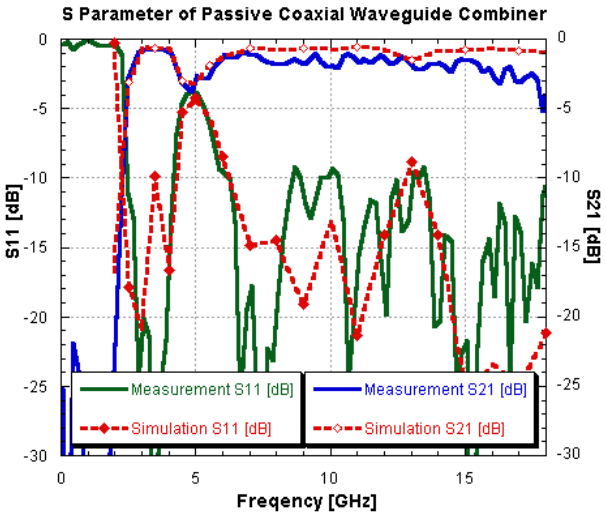

Fig. 8. Comparisons between simulation and measurement for passive coaxial waveguide combiner.

VI. Conclusion

A compact coaxial waveguide combiner structure is presented in this paper. The total size of the new system is reduced dramatically compared to previous ones. And with the monolithic integration of the microstrip to slotline transition, fabrication of the system becomes easier with same performance. Furthermore, the new transition makes it possible to extend the structure to higher frequencies.

Acknowledgement

The authors wish to acknowledge the assistance and support of Paolo F. Maccarini. This work is funded through the ONR MURI IMPACT program (grant N00014-96-1-1215), and by an ARO MURI program (grant DAAG55-98-1-0001).

References

[1] N. –S. Cheng, P. Jia, D. B. Rensch and R. A. York, "A 120-Watt X-Band Spatially Combined Solid-State Amplifier", *IEEE Trans. Microwave Theory and Tech.*, Vol. MTT-47, No.12, pp. 2557-61, Dec 1999.

[2] P. Jia, L.-Y. Chen, N.-S. Cheng, and R.A. York, "Design of Waveguide Finline Arrays for Spatial Power Combining", to be published on *IEEE Trans. Microwave Theory and Tech*, April 2001.

[3] P. Jia, Y. Liu, R.A. York, "Analysis of A Passive Spatial Combiner Using Tapered Slotline Array in Oversized Coaxial Waveguide", *2000 IEEE MTT-S International Microwave Symposium Digest*, Boston, MA, USA, pp.1933-6, Vol.3, June 2000.

[4] P. Jia, L.-Y. Chen and R.A. York, "Ultra-Broadband Coaxial Waveguide Power Combiner", submitted to *IEEE Trans. Microwave Theory and Tech.*.

[5] D. M. Pozar, *Microwave Engineering*, 2nd Ed., New York, NY: John Wiley & Sons, 1998.

[6] R.W. Klopfenstein, "A Transmission-Line Taper of Improved Design," *Proc. IRE*, vol. 442, pp. 31-35, January 1956.

[7] M.M. Zinieris, R. Sloan, and L.E. Davis, " A Broadband Microstrip-To-Slot-Line Transition", *Microwave and Optical Technology Letters*, vol 18, No. 5, pp 339-342 August 1998.

[8] B. Schuppert, "Microstrip/Slotline Transitions: Modeling and Experimental Investigation", IEEE *Trans. Microwave Theory and Tech.*, Vol. 36, 1988, pp. 1272-1282.

[9] K.C. Gupta, R. Garg, and I.J. Bahl, *Microstrip Lines and Slotlines*, Artech House, Norwood, MA, 1979.